Prediction of Liquefaction from a Viewpoint of Strain Energy

Department of Civil Engineering,
Faculty of Engineering, Tohoku University
Eiji YANAGISAWA, Prof. Dr.

1. Introduction

The liquefaction phenomenon of sandy soils during earthquake excitation is one of the serious problems in earthquake geotechnical engineering. Generally, the conventional method of liquefaction prediction is based on the multiple reflection theory of shear waves and the equivalent linear assumption in shear deformation. In the design of foundation on a liquefiable ground, the maximum ground surface acceleration are given to the construction site, and liquefaction susceptibility is estimated from the liquefaction safety factors, which are defined by the ratio of undrained shear strength of soils and dynamic shear stress induced by the seismic waves. However, in liquefied state, soils can no longer sustain the earthquake loads, and amplification of seismic waves results in decrease in the response acceleration of the ground surface.

After the Hyogokenn-Nambu Earthquake, it is pointed out that studies on the dynamic strength of soils to a larger loading level than ever are needed not only for clean sand but also a wide variety of soils with a wide range of grading. The authors proposed a method of liquefaction prediction based on an index which is defined by accumulated dissipation energy which has been consumed in the process of plastic deformation under repeated loading condition during the earthquake. The ways of increase in accumulated dissipation energy and reduction of the shear modulus by pore pressure are keys to estimate the liquefaction strength of soils. The method has the advantage of simplicity to take the ductility and plastic deformation characteristics into account and to express the degree of deterioration of soil layers by the earthquake.

In order to predict the liquefaction susceptibility, it is needed to evaluate the external seismic force in terms of an amount of dissipation energy consumed by the plastic deformation in a soil element. This study deals with a simple method of liquefaction prediction, in which the accumulated strain energy is used to evaluate the generation of pore pressure and the reduction of the shear modulus in the horizontal soil layers. Then the effects of seismic excitation forces on liquefaction are also studied. In this context, the evaluation of seismic excitation forces means the prediction of influence of input earthquake waves to the soil layers from the view point of strain energy theory. By use of these assumptions we can explain the reasons why the damage of earthquake differs from an earthquake to another, whose maximum acceleration at the ground surface reached to almost the same level , for example, more than 500gals. The author has

already discussed in the previous paper how the influences of seismic forces differ from the other by comparing the strong earthquake records observed during the Hyogoken-Nambu Earth-quake and the Sanriku Harukaoki Earthquake. From previous studies it is pointed out that it is quite difficult to find out the most influential factors of earthquakes and that the maximum acceleration is not always the only parameter which is essential to cause the liquefaction. In this study, the influential factors of the earthquakes are studied by comparing the re-sponses of the ground to various input waves.

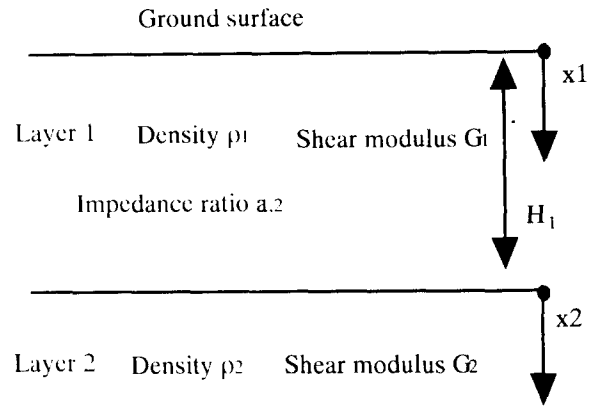

Figure 1. Horizontal layered ground.

A few studies have been made so far on the influence of earthquake waves to liquefaction from viewpoint of energy. Towhata et al proposed a method to predict the liquefaction by utilizing the Spectrum Intensity (SI) obtained from the earthquake records on the ground surface. In this case Towhata calculated the Spectrum Intensity by an equation as follows.

$$SI_{h=20\%} = \frac{1}{2.4}\int_{0.1}^{2.5} S_{v\,h=20\%}\, dT \qquad \text{[cm/s]} \qquad (1)$$

Since the SI is a quantity which corresponds to seismic input energy, it might be possible to predict the occurrence of liquefaction on the bases of the strain energy. Actually, it is already found out so far from the element tests, that the generated pore pressure is closly related to the accumulated strain energy irrespect to the testing apparatus. Namely, the pore pressure ratio can be defined by an unique function of the accumulated dissipation energy normalized by the hydrostatic pressure regardless of the testing methods and loading conditions. It is also pointed out that in a specific state of density of sand, the initial liquefaction will occur when the accumulated dissipation energy reaches to a definite value. The authors performed strain controlled cyclic loading tests on the various kinds of soils and compared the accumulated strain energy. From the test results we found out that there exists a limiting value of the accumulated strain energy for the liquefiable sandy soils, whereas the strain energy for cohesive soils increases monotonically because there is no reduction in the shear modulus. This can be recognized as a characteristic of the non-liquefiable soils.

2. Incident seismic energy to surface layer

Consider a simple case of horizontal two-layered system as shown in Figure 1, namely a horizontally sedimented surface layer on a bed rock. Transmission of the energy by incident SH

waves will be discussed hereafter. Assumed that the materials are linear elastic and sinusoidal wave of angular frequency of ω was transmitted vertically from the bed rock, the steady state response amplitude at a distance x_n from the surface can be stated from the equation (2)

$$u_n(x_n,t) = (E_n e^{ik_n x_n} + F_n e^{-ik_n x_n}) e^{i\omega t} \tag{2}$$

where u_n : displacement in the n-th layer, E_n: amplitude of the incident wave in the n-th layer, F_n: amplitude of the reflection wave in the n-th layer, k_n: wave number defined from the angular frequency of the wave and the shear wave velocity of the n-th layer, t: time in second.

Taking into account the stress free condition at the ground surface and the continuity condition of force and displacement at the boundaries between two adjacent layers, the displacement amplitude of refraction wave and reflection wave in each layer can be obtained as follows,

$$F_1 = E_1 \tag{3}$$

$$E_2 = \frac{1}{2}E_1\left\{(1+\alpha_{1,2})e^{i\beta_1} + (1-\alpha_{1,2})e^{-i\beta_1}\right\} \tag{4}$$

$$F_2 = \frac{1}{2}E_1\left\{(1-\alpha_{1,2})e^{i\beta_1} + (1+\alpha_{1,2})e^{-i\beta_1}\right\} \tag{5}$$

in which α : an impedance ratio, H_1: thickness of the surface layer, β_1: nondimensional wave number k_1H_1, ρ: density, G: shear modulus of the layer.

From the amplitude of each wave, the kinematic energy K and elastic strain energy P can be written in the form

$$K = \frac{1}{2}\rho v^2 = \frac{1}{2}\rho\left(\frac{\partial u}{\partial t}\right)^2 \tag{6}$$

$$P = \frac{1}{2}G\gamma^2 = \frac{1}{2}G\left(\frac{\partial u}{\partial x}\right)^2 \tag{7}$$

Substituting Eq.(2) to Eqs.(6) and (7), the kinematic energy and strain energy at a point can be expressed as follows.

$$K_1 = 2\rho_1\omega^2 E_1^2 \sin^2\omega t\cos^2 k_1x_1 \tag{8}$$

$$P_1 = 2G_1k_1^2E_1^2\cos^2\omega t\sin^2 k_1x_1 \tag{9}$$

$$K_2 = 2\rho_2\omega^2E_1^2\sin^2\omega t(\cos\beta\cos k_2x_2 - \alpha\sin\beta\sin k_2x_2)^2 \tag{10}$$

$$P_2 = 2G_2k_2^2E_1^2\cos^2\omega t(\cos\beta\sin k_2x_2 - \alpha\sin\beta\cos k_2x_2)^2 \tag{11}$$

By averaging the Eqs (8) to (11) by the time interval T, we can define the average kinematic energy $\overline{K}$, the average strain energy $\overline{P}$ and average total energy $\overline{T}$ for unit volume of soils in an arbitrary depth of the layers.

$$\overline{K}_1 = \rho_1 \omega^2 E_1^{\,2} \cos^2 k_1 x_1 \tag{12}$$

$$\overline{P}_1 = G_1 k_1^{\,2} E_1^{\,2} \sin^2 k_1 x_1 \tag{13}$$

$$\overline{T}_1 = \overline{K}_1 + \overline{P}_1 = \rho_1 \omega^2 E_1^{\,2} \tag{14}$$

$$\overline{K}_2 = \rho_2 \omega^2 E_1^{\,2} (\cos\beta \cos k_2 x_2 - \alpha \sin\beta \sin k_2 x_2)^2 \tag{15}$$

$$\overline{P}_2 = G_2 k_2^{\,2} E_1^{\,2} (\cos\beta \sin k_2 x_2 - \alpha \sin\beta \cos k_2 x_2)^2 \tag{16}$$

$$\overline{T}_2 = \overline{K}_2 + \overline{P}_2 = \rho_2 \omega^2 E_1^{\,2} (\cos\beta - \alpha^2 \sin\beta)^2 \tag{17}$$

$$\frac{\overline{T}_1}{\overline{T}_2} = \frac{\rho_1}{\rho_2} \frac{1}{(\cos\beta - \alpha^2 \sin\beta)} \tag{18}$$

Figure 2 indicates the distribution of energy defined by the Eqs.(12) to (17), when the impedance ratio α is assumed to be 0.5. From this figure it is observed that kinematic energy and strain energy show different distribution curves in the direction of the depth. However, the total energy takes always the same value throughout the surface layer, whose value is given by a function of the impedance ratio α and nondimensional wave number β. It should be noted that only kinematic energy exists at the ground surface and on the other hand only potential energy exists at the point of a node of the waves. The ratio of total energy of surface layer to the base rock can be designated by Figure 3. From this figure it is easily understand that amplification occurs when α is smaller than unity and deamplification will be seen α becomes less than unity. Resonance of the ground will occur when the surface layer is shaken by the wave with the period of 4H/Vs, as is predicted by the multiple reflection theory.

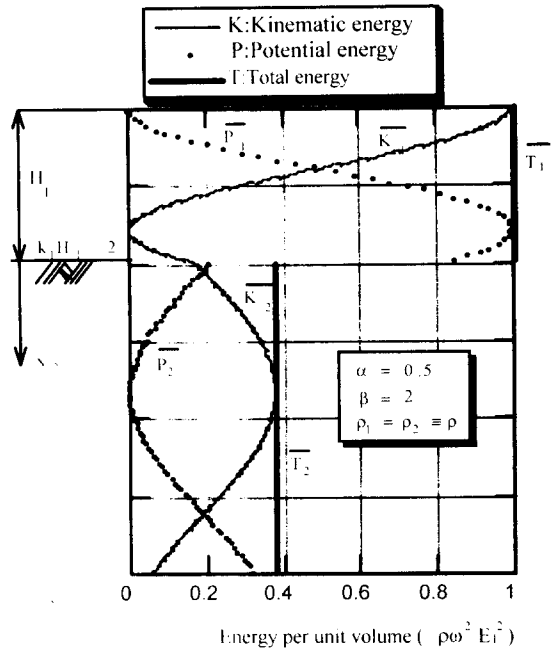

Figure 2. Distribution of the energy in depth direction.

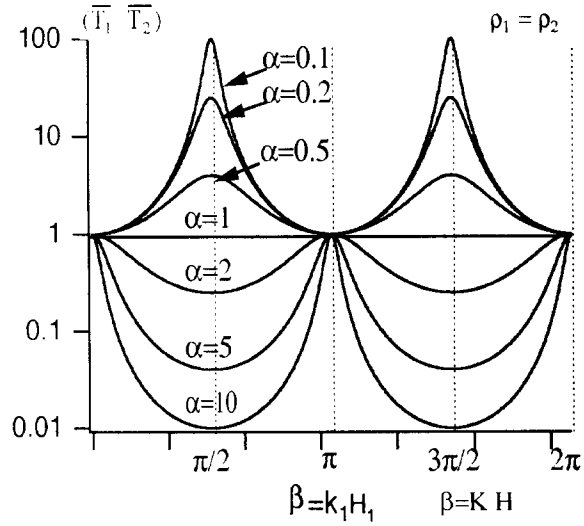

Figure 3. Relation among the energy ratio, the impedance ratioα and non-dimensional wave number β.

If we apply the results mentioned above to the multi-layered system, we will see how the distribution of total energy will be affected by the soil structure. In addition to that the distribution of kinematic energy and potential energy will vary, if the structure of soil layers is

changed. Therefore in order to evaluate the incident energy to the ground at a site, the soil layers at the specified site must be assumed and then the seismic response of the layer system will be calculated.

In the previous section, the ground is assumed to be linear elastic. However in the cases of strong earthquakes, soil materials usually deform to a plastic state and energy is consumed during seismic loading cycles which are often referred as hysteretic damping energy or dissipation energy. In this paper the dissipation energy which is accumulated during the cycles of repeated loading due to seismic forces is defined as accumulated dissipation energy. The accumulated dissipation energy can be calculated from the area between loading path and unloading path of stress strain relationship.

$$\Delta w = \oint_f \tau(\gamma) d\gamma = \int_0^t \tau(\gamma)\dot{\gamma} dt \qquad (19)$$

In the equivalent linear analysis, because of linearity assumption there is no way to calculate the nonlinear plastic deformation. However from the time histories of the equivalent linear analyses the elastic strain energy which is stored in a element at a certain depth can be calculated by the Equation (20), where G_{eq} is the equivalent shear modulus.

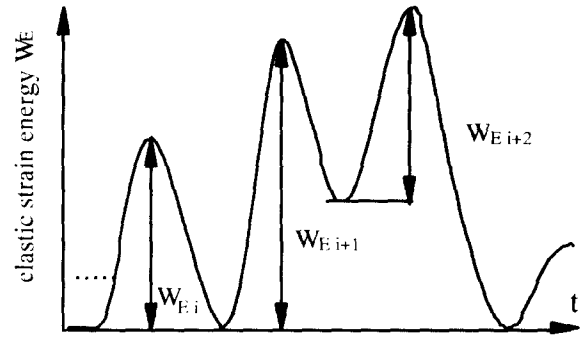

Figure 4. Schematic diagram of the time history of elastic strain energy accumulated in the soil subjected to random loading.

Table 1. Model ground used in this study.

Layer NO.	Height K.P.(m)	Ground type	Thickness (m)	Unit Weight (tf/m^3)	Vs (m/s)
1	4	Reclaimed material	2.0	1.7	170
2	2	Reclaimed material	2.0	1.7	170
3	0	Reclaimed material	1.0	2.0	210
4	-1	Reclaimed material	1.0	2.0	210
5	-2	Reclaimed material	1.0	2.0	210
6	-3	Reclaimed material	1.0	2.0	210
7	-4	Reclaimed material	1.0	2.0	210
8	-5	Reclaimed material	1.0	2.0	210
9	-6	Reclaimed material	2.0	2.0	210
10	-8	Reclaimed material	2.0	2.0	210
11	-10	Reclaimed material	2.0	2.0	210
12	-12	Reclaimed material	1.4	2.0	210
13	-13.4	Alluvial clay	2.6	1.6	180
14	-16	Alluvial clay	2.0	1.6	180
15	-18	Alluvial clay	2.0	1.6	180
16	-20	Alluvial clay	2.0	1.6	180
17	-22	Alluvial clay	2.2	1.6	180
18	-24.2	Diluvial layer	1.8	2.0	245
19	-26	Diluvial layer	2.0	2.0	245
20	-28	Basement ground		*	*

$$W_L(t) = \frac{1}{2} G_{eq} \{\gamma(t)\}^2 \qquad (20)$$

Damping ratio is usually defined from a hysteretic curve. However, in this paper, the difference in elastic energy stored between one loading point and the other peak point, is assumed as the dissipation energy as is shown in Figure 4.

$$h_{eq} = \frac{1}{2\pi}\frac{\Delta w}{W_E} \tag{21}$$

Table 2.Earthquake wave used in this response analysis .

No	Year	Earthquake	Location of observation	Direction	In put wave	Max.Acc (Gal)	Max.Acc *3	Number of data	Density (t/m^3)	Velocity of Swave (m/s)
1	1968	Tokachi	Hachinohe port	NS	Incident wave	170	153	1800	2.00	380
2	1978	Miyagi Ken-Oki	Ouhunato port	E41S	Incident wave	161	158	1800	2.00	650
3			Kaihokubasi	W42N	Incident wave	293	279	1800	2.00	650
4	1993	Kusiro-Oki	Kusiro port	EW	Incident wave	221	221	3600	1.80	430
5	1994	Hokaido Nansei Nansei-Oki	Hakotate Port	N03W	Incident wave	142	142	7200	1.84	550
6			Muroran Port	EW	Incident wave	144	144	7200	2.00	420
7	1994	Sanriku-Oki*1	Hachinohe Port*2	EW	Incident wave	1350	1350	3600	2.00	341
8	1995	Hyogo Ken*1	Koube PI	NS	Observation	544	504	1800	2.00	305

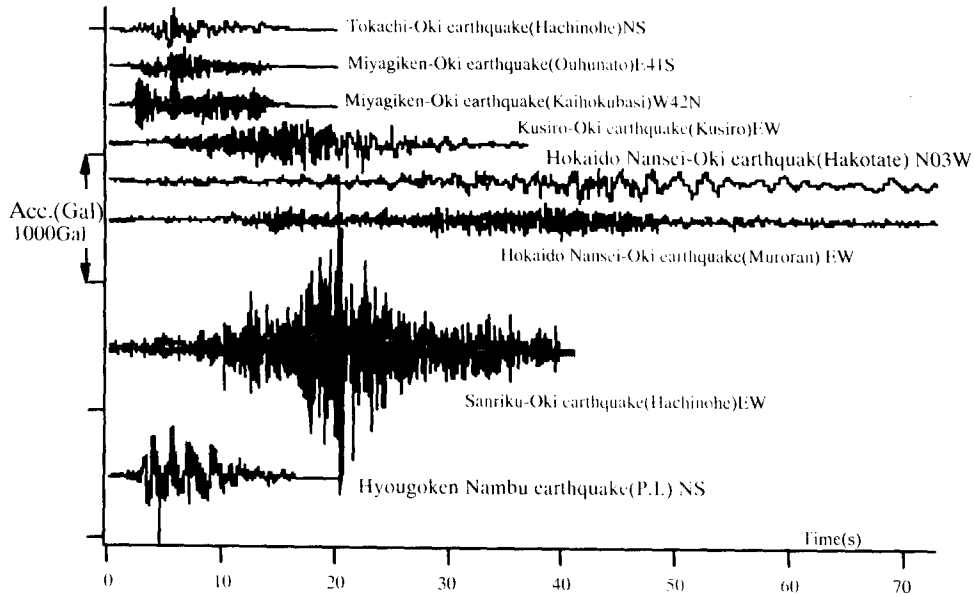

Figure 5. Time histories of incident base motion used in the response anaiysis.

By drawing the time history of the elastic energy stored in each layer, accumulated dissipation energy can be obtained by adding the energy difference at the peak of each cycle of loading. In this study, however, the damping ratio is assumed to be constant throughout a sequence of an earthquake.

3. Method of Response Analysis

We take an example of the ground condition of the array observation site in Kobe Port Island, Japan. The ground consists of three layers of reclaimed material, alluvial clay and diluvial gravel on a bed rock. In the array observation system, seismometers are installed to the depth of -79m below sea level, however in this study we take the ground condition into consideration only to

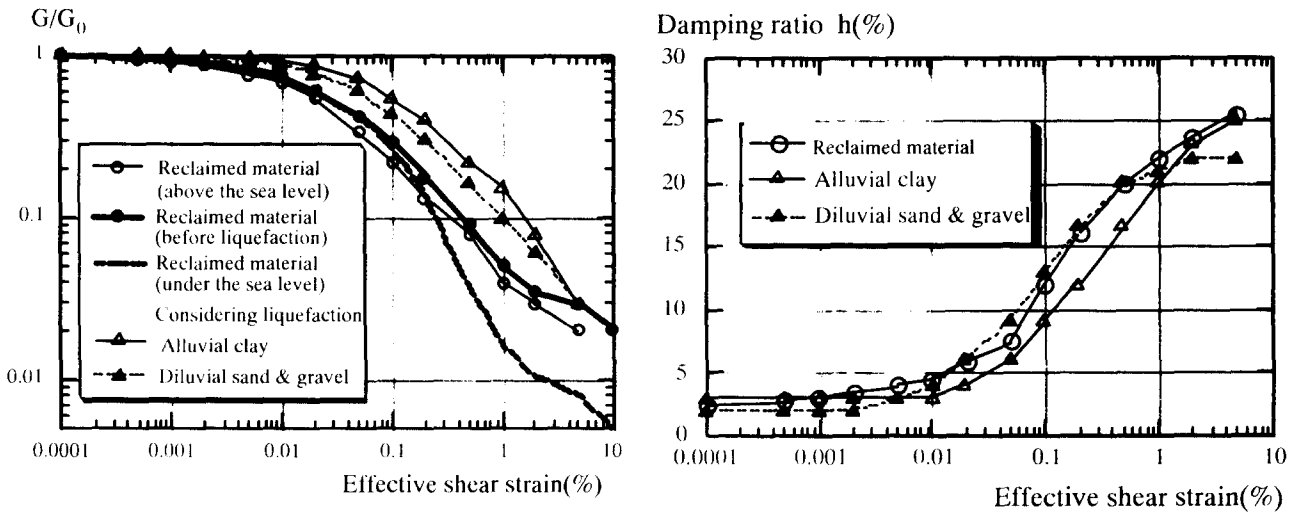

Figure 6. Shear modulus and damping dependency on strain amplitude.

the depth of -28m, because nonlinearity appears significantly in these two soft layers. Table -1 shows the subdivision of layers, which are used for the study, based on the survey data referred to the report from the authorities of Kobe City.

For this analysis, eight earthquake records of a horizontal component observed during six different strong earthquakes are chosen in which the maximum accelerations have been observed. In order to eliminate the effect of ground conditions in each site, input waves are calculated from these observed records by use of the SHAKE program assuming a strain dependency curve used in the standards of the Ministry of Transportation. Figure 5 shows the input waves used in this study. At a glance into this figure peculiar characteristics of waves can be recognized in the record of Sanriku-Harukaoki Earthquake in terms of the maximum acceleration and duration time. In order to clarify the difference in the responses of the ground shaken by different input earthquake waves, the material constants of the bed rock are assumed to be the ones of the bed rock of each observation site. This means that in the case of Sanriku Harukaoki Earthquake, for example, the soil strata of Port Island were assumed to be lying on the bed rock of the Hatinohe Harbor and then the input wave calculated from the seismic records at the Hachinohe Harbor was applied through the base rock to the soil strata. Response was calculated by equivalent linear analysis where Fourier transformation was used to change the waves from time domain to the frequency domain and vice versa. The maximum frequency used in this analysis was up to 10Hz.

Figure 6 shows the strain dependency of the shear modulus and damping ratio which has been studied by the authorities of the Kobe City. From the results of strain controlled triaxial undrained tests, it can be said that the reduction in the shear modulus of reclaimed material due to pore pressure generation should be taken into account for larger strain than 0.1%. For the simplicity, reduction of the shear modulus was estimated from the results of cyclic triaxial test, in

which the stress strain curve at the fourth cycle of loading was taken to evaluate the dynamic constants because the Hyogoken-nambu Earthquake has four predominant peaks in the waves.

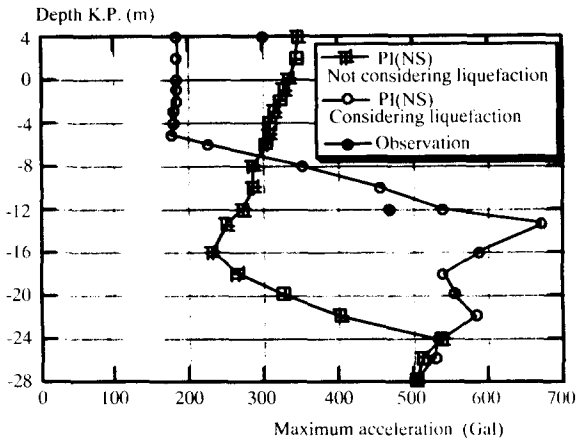

Figure 7. Distribution of the maximum acceleration in depth direction. (Hyogoken Nambu earthquake, NS component of Kobe Port-Island)

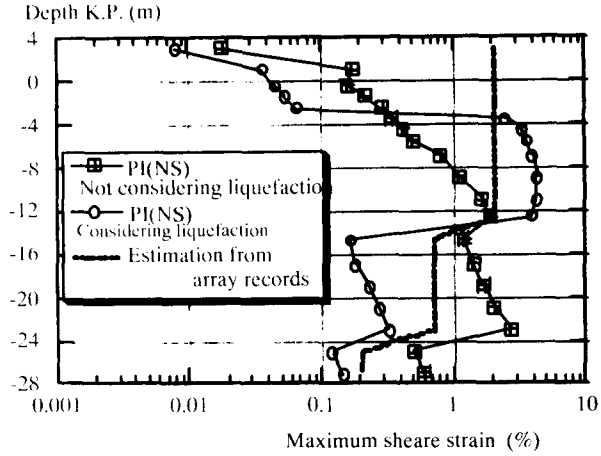

Figure 8. Distribution of the maximum shear strain in depth direction. (Hyogoken Nambu earthquake, NS component of Kobe Port-Island)

Then the specific reduction curve for liquefaction state was obtained by revising the reduction curve of the reclaimed material in saturated state or under sea level, which is designated by dotted line in the Figure 6. Concerning to the damping ratio of the reclaimed materials, most of test results coincide approximately with the reduction curve of sands and the effects of saturation are not clearly detected by the tests so far. Then the curves for sands are used in the calculation instead of the curve of the reclaimed materials, because there is a lack of data in larger strain for the cases of the reclaimed materials.

As is well known, during the Hyogoken Nambu Earthquake, strong motion records were obtained by the array observation system at a site of Kobe Port Island. By comparing the calculation results to observed ones, validity of assumptions of equivalent linearity and strain dependency can be evaluated. Figures 7 to 9 are the calculation results of equivalent linear analyses with and without the effect of liquefaction, when the observed wave of the Hyogoken-Nambu Earthquake at the depth of -28m was directly used as an input wave. Regarding Figure 7, although two kinds of analyses result in different shapes of distribution of the maximum acceleration, tendency of reduction of acceleration in the liquefied layers seems to coincide with observed one. If liquefaction is not taken into account, the maximum acceleration should be larger at the ground surface than at -12m point. Shear strain distributions obtained from these analyses are plotted in Figure 8. From the figure, if the effect of liquefaction is neglected, larger strain appears in the clay layer and smaller in reclaimed materials. If the effect of liquefaction is taken into consideration then the strain in the reclaimed material become larger compared with one in the clay layer. In the same figure, the average maximum acceleration estimated directly

from array observation records is shown by the solid line. In this case the maximum acceleration in the reclaimed materials are found to be larger than the ones in the clay layer. In this sense the

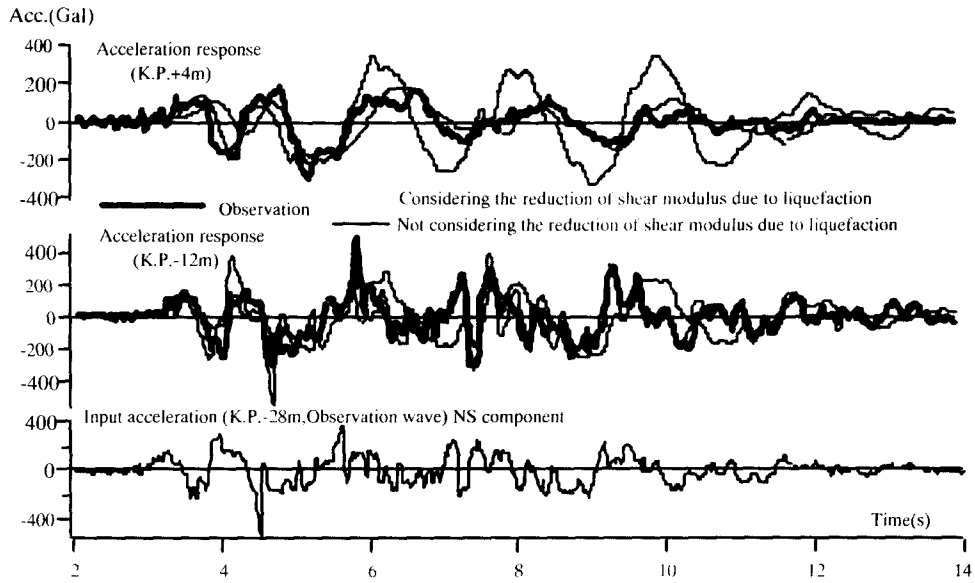

Figure 9. Comparison time histories of observed the equivalent linear with the motion

tesndency of strain distribution of the liquefied case resembles more to the observed values rather than the case of nonliquefied state. Therefore, it can be said that the better approximation can be obtained by assuming the shear modulus curve of reclaimed material as it was liquefied. Regarding to the time history of Figure 9 the observed record at the ground surface is well approximated by the calculation results of the case in which liquefaction is assumed.

From these facts mentioned above, the responses of the ground at Kobe Port Island can be reasonably simulated by the equivalent linear analyses in which the effect of the reduction in the shear modules of reclaimed materials is taken into account. There have been done so far a few studies to simulate the observed array records by equivalent linear analyses. Sato et al, for example, have studied changes in the shear modulus and damping ratio by means of back analysis and tried to simulate the response of the ground by use of the strain dependent characteristics determined by the back analyses. Miwa has studied also the array records and shown that the equivalent linear analyses can be used when the strain dependency curves are properly given for each layers.

4. Responses of the ground to various input waves

The responses of the ground to various input waves with the same soil profile as the Kobe Port Island are studied as well. Figure 10 shows the calculation results of distribution of the maximum acceleration from the surface to the depth of -28m. All the results shown in this figure are

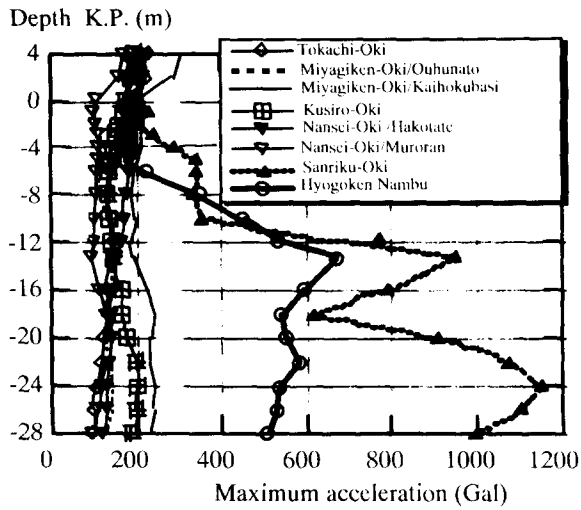

Figure 10. Distribution of the maximum acceleration response in depth direction.

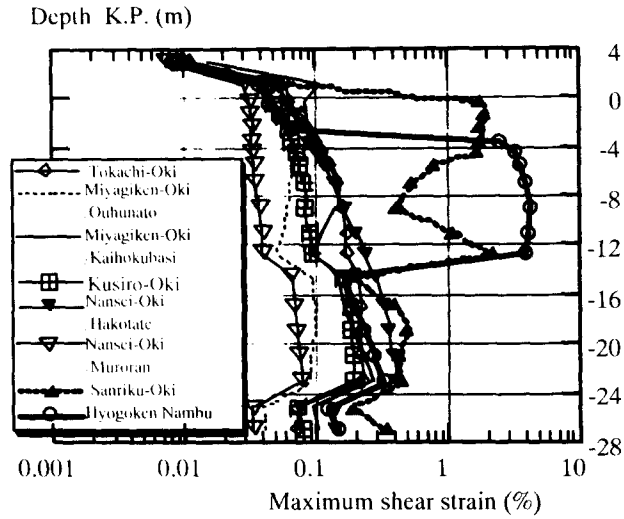

Figure 11. Distribution of the maximum shear strain in depth direction.

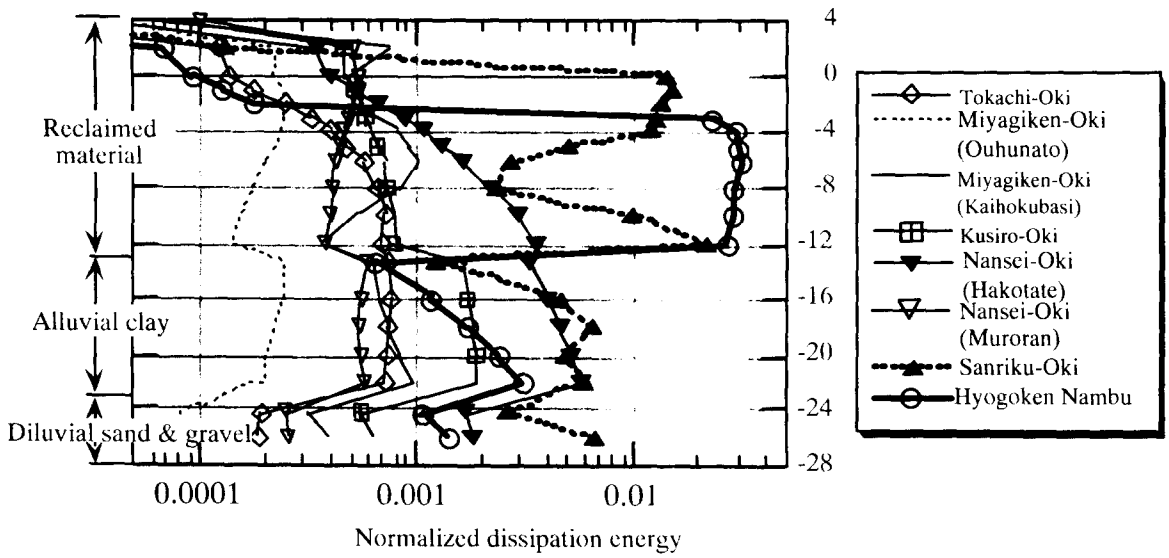

Figure 12. Distribution of the normallized dissipation energy in depth direction.

obtained under the condition that the shear modulus of reclaimed materials has been assumed as it takes the values of liquefied state. It can be seen from this figure that for most of the earthquakes such as Tokachioki-oki earthquake and Miyagiken-oki earthquake the response is slightly amplified at the surface by the layers of soils. However, in the cases of larger earthquakes, such as Hyogoken-Nambu Earthquake and Sanriku Haruka-oki Earthquake the maximum acceleration at the surface decreases significantly due to the reduction of the shear modulus of the reclaimed materials. Comparing time histories of the response to these two

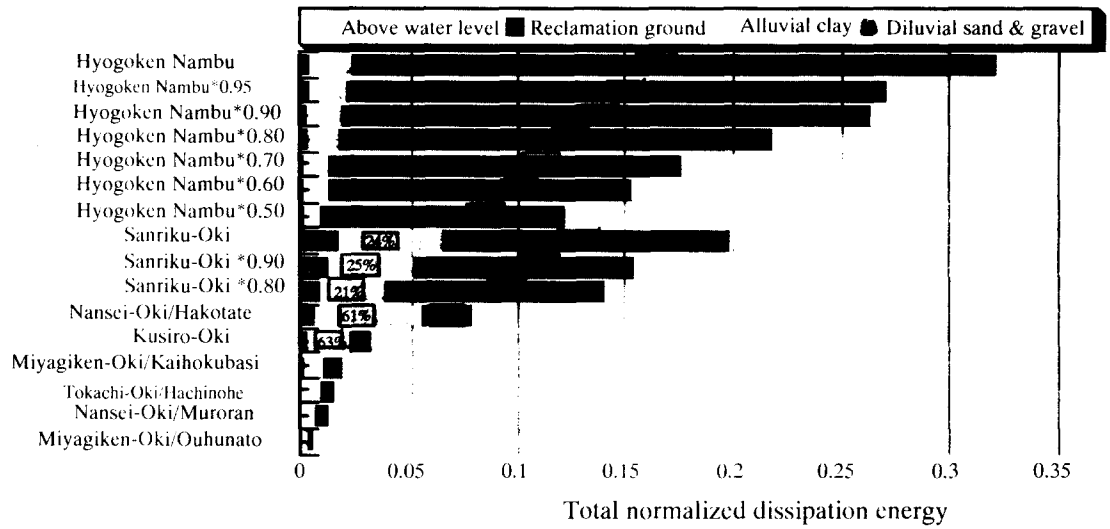

Figure 13. Total normallized dissipation energy and percentages for various earthquake motions.

earthquakes from the depth to the surface, it can be seen that the waves of rather high frequency components disappear gradually as the depth decreases. Sudden decrease in the maximum acceleration and vanishing of the higher frequency component in the waves imply the possibility of liquefaction.

Figure 11 shows the distribution of the maximum shear strain in the soil layers. It should be noted that the shear strain was evaluated at the middle point of each layer element. Looking at the figure it is easily recognized that the response strains to incident waves of Hyogoken-Nanbu Earthquake and Sanriku Haruka-oki Earthquake indicate considerably larger values to the extent of several percent in the layer of reclaimed materials. On the contrary, the maximum strain induced in the same layer remains less than 0.2% by the other earthquakes than the above two, and therefore the maximum strains in clay layer become larger than the ones in the reclaimed materials. Similar tendency can be seen in Figure 12, in which the distributions of accumulated dissipation energy normalized by the overburden pressure are plotted for different earthquakes. Larger energy dissipation is seen in the reclaimed materials when the ground was shaken by the two strongest earthquakes, Hyogokenn-Nambu Earthquake and Sanriku Haruka-oki Earthquake. These tendencies are considered to be caused by the fact that the initial shear modulus of the clay layer is smaller than that of the reclaimed materials and then the response becomes larger when it was shaken by rather small amplitude. However if the shaking becomes so large that the liquefaction occurs in the reclaimed materials, then the shear strain becomes larger than that of clay layer because substantial reduction of the shear modulus occurs in the reclaimed materials due to pore pressure generation. In figure 13, the comparison of proportion of accumulated dissipation energy consumed in each layer of soils are shown in percent of total sum of them. In

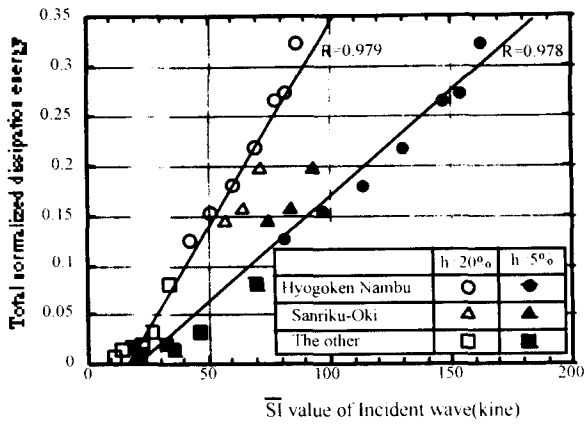

Figure 14. Relation between the SI value (Incident wave) and dissipation energy.

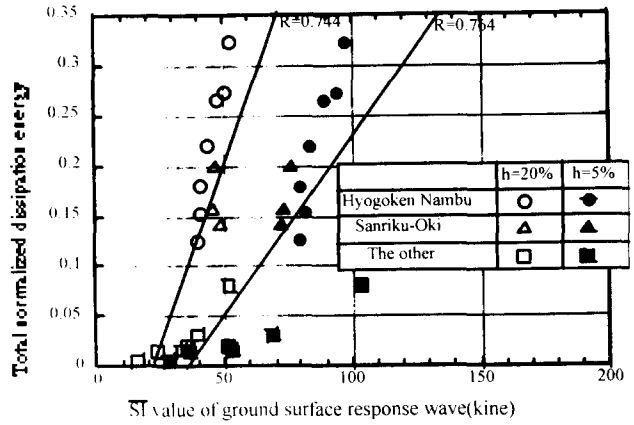

Figure 15. Relation between the SI value (Response wave) and dissipation energy.

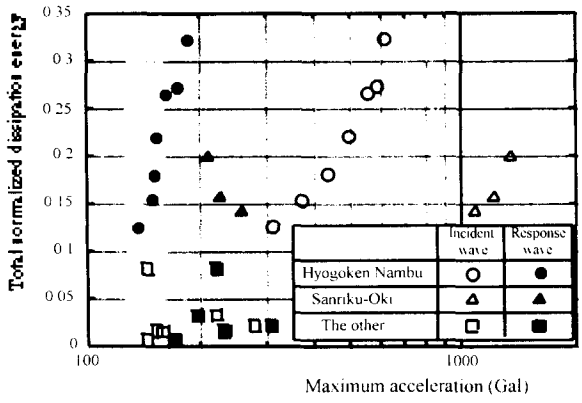

Figure 16. Relation between the maximum acceleration and dissipation energy.

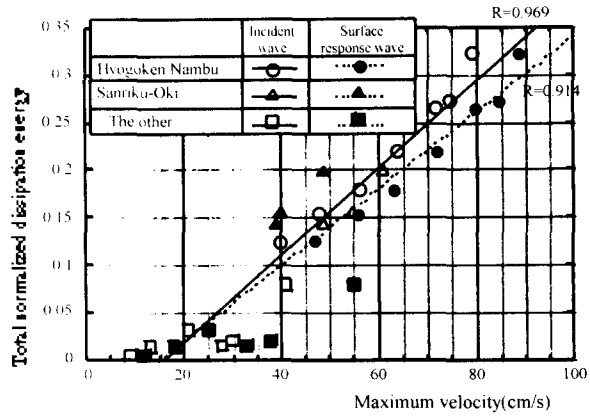

Figure 17. Relation between the maximum velocity and dissipation energy.

the same figure, the calculation results for input waves whose amplitude was reduced by 95% to 50% of the original wave are shown. It is recognized from this figure that in the case of Hyogoken-Nambu Earthquake 93% of total dissipation energy was consumed in the reclaimed material, while in the case of Sanriku Haruka-oki Earthquake 67% of the dissipation energy is worked by the deformation in the reclaimed soils. The proportion of the dissipation energy changes when the input wave is changed. However, for the reduced waves shown in the same figure, the proportion of the energy dissipation in the reclaimed layer decreases linearly in proportion to the percentage of the reduction. This means that the proportion of energy dissipation in each layer can be attributed to the specific features of input earthquake waves.

In order to find out adequate indices which can be directly related to accumulated dissipation energy, specific features of the earthquake waves, such as spectrum intensity (SI), the maximum acceleration and the maximum velocity, were chosen and studied how they will affect

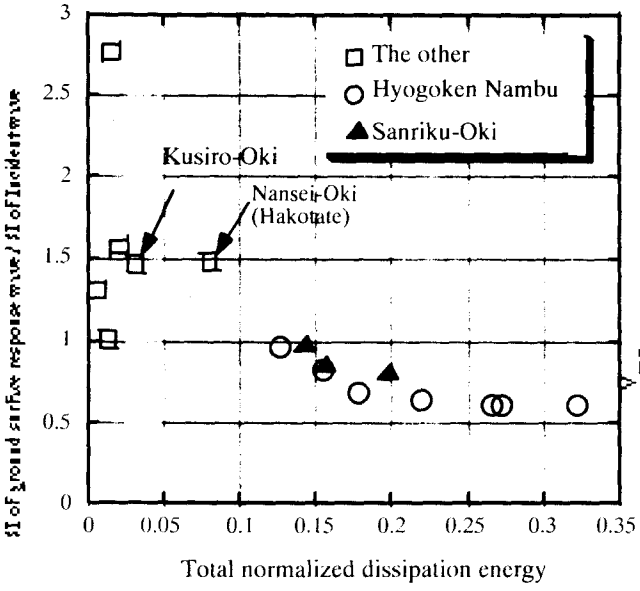

Figure 18. Relation between the dissipation energy and ratio of SI value.

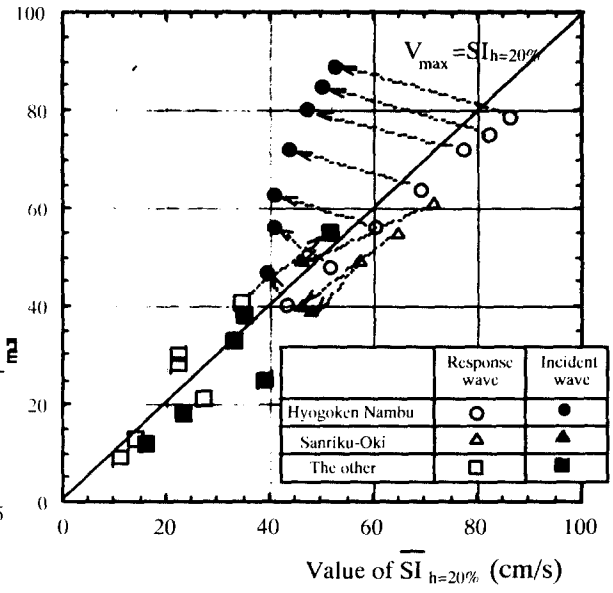

Figure 19. Relation between the maximum velocity and ratio of SI value(h=20%).

the response. In this paper, the spectrum intensities of both waves were calculated on the response at the surface of the ground and the input wave at the bed rock with the damping ratio of 5% and 20%.

Equation (2) was used to obtain SI values which were proposed by Towhata et al to compare the results with previous studies. In Figures 14 and 15, the relation between total sum of accumulated dissipation energy in the ground and SI values are shown for the cases of input waves at the base rock and response waves at the ground surface. Figures 16 and 17 indicate the relation of the maximum acceleration as well as the maximum velocity to the total accumulated energy dissipation in the whole ground system. Time history of velocity in this case was obtained by integrating each frequency components after filtering the low frequency components below 0.15Hz by use of low cut filter in frequency domain. It can be seen from these figures that the highest correlation was obtained in the case of the relation of SI values of input waves at the base rock, in which the coefficient of correlation was calculated to be 0.979. Similar tendency was seen in the case of 5% damping, and it was found that the effect of damping ratio is negligibly small. However, for the cases of SI values of the responses at the ground surface, the coefficient of correlation will drop to 0.74 for 20% damping and 0.76 for 5% damping. It can be said from these results that the prediction of liquefaction from the SI values calculated at the ground surface does not always give correct answer. Although the correlation between the maximum acceleration and the dissipation energy can be seen for each earthquake, strong correlation can

not be seen for all of the earthquakes as a whole. On the other hand the maximum velocity shows good correlation to the dissipation energy for all of earthquakes and the correlation coefficient reaches to 0.969 for the input waves and 0.917 for the responses at the ground surface.

c) Reduction of SI value by softening of the surface soil

Figure 18 indicates the relation between the accumulated dissipation energy and the ratio of the SI value of the surface response to the SI value of the input wave. It can be seen from this figure that the larger the accumulated dissipation energy is, the smaller the ratio becomes. The ratio becomes less than unity when the dissipation energy increases. The actual meaning of the ratio of less than unity is that the input earthquake force is much stronger than that of response at the ground surface, therefore it can be said that the soil layer worked as isolation equipment by the softening of materials.

According to Towhata et al, the maximum velocity at the surface of the ground is approximately equal to the SI values with 20 % damping. Figure 19 shows the relation of theses two values obtained in this study. Most of the points located around the linear line of $SI_{20\%}=V_{max}$, but for the cases of the SI at the surface of the ground. Because of effect of liquefaction, Vmax becomes larger, while the SI value reduces. Therefore it should be noted that if the liquefaction is predicted from the surface response then there is a possibility of underestimation.

5. Conclusions

In this study, the severity of earthquakes is evaluated by responses of the surface layers to strong earthquake records which may cause liquefaction in reclaimed materials and the effects of wave characteristics were studied in the viewpoint of accumulated dissipation energy. The conclusions can be made as follows.

(1) Strain dependency curves of the shear modulus and damping ratio for reclaimed materials are assumed by taking the reduction of the shear modulus due to pore pressure into consideration, and then the equivalent linear analyses are performed on the layered model of the ground at the site of array observation system in Kobe Port Island. As a result, even in the case of nonlinear behaviors of soils as liquefied state, the equivalent linear analysis is enough accurate when the reduction of the shear modulus due to liquefaction is adequately evaluated.

(2) A method to estimation the accumulated dissipation energy is proposed to evaluate the amount of energy exhausted in the layers during the earthquakes.

(3) Taking the model of soil layers of Kobe Port Island for example, the responses of the ground to the various strong earthquakes are obtained, and the accumulated dissipation energy in each soil layers is evaluated. It is found from these results that the dissipation energy is closely related to the maximum strain and the total sum of the dissipation energy in each soil layer can be used as a damage parameter which indicates the degree of plasticizing of soils by the earthquakes. In

the context of the severity of earthquake, the order of the earthquake is found to be the Hyogoken-Nambu Earthquake, Sanriku-Harukaoki Earthquake, Hokkaido-Nanseioki Earthquake, and so on.

(4) The values of spectrum intensity and the maximum velocity have a strong correlation to the total sum of dissipation energy worked in the ground, but the maximum acceleration has a very weak correlation to the dissipation energy. Moreover a higher correlation coefficient is obtained when the SI is calculated by the input waves rather than by the response at the ground surface.

(5) In this paper the response analysis is limited to the equivalent linear method, however, the method based on the dissipation energy has an advantage of possibility of wide range of application from nonlinear liquefaction analysis to post failure analyses of liquefied soils.

REFERENCES

Housner G.W.: Behaviour of structure during earthquakes, *ASCE, EM4*, pp.109- 129, 1959.

Housner G.W.: Limit design of structure to resist earthquakes, *Proc. of 1st. WCEE*, pp.1-13, 1956.

Towhata, I., Park, J.K., Orense, R. P. and Kano, H.: Use of spectrum intensity for immidiate detection of subsoil liquefaction, *Soils and Foundations*, Vol.36, No.2, pp.29-44, 1996.

Sugano,T. and Yanagisawa,E. : Undrained shear behavior of sand under surface wave stress conditions, *Proc.of the 9th.Asian Regional Conf. on Soil Mechanics and Foundation Engineering*, Vol.1, pp.71-74, 1991.

Sugano,T. and Yanagisawa,E. : Cyclic undrained shear behavior of sand under surface wave stress

conditions, *Proc.of the10th.WCEE*, Vol.3, pp.1323-1327, 1992.

Towhata, I. and Ishihara, K.: Shear work and pore water pressure in undrained shear, *Soils and Foundations*, Vol.25, No.3, pp.73-84,1985.

Okada, N. and Nemat-Nasser, S. : Energy dissipation in inelastic flow of saturated cohesionless granular media, *Geotechnique*, Vol.44, No.1, pp.1-19, 1994.

Kazama, M.*et al.* : Liquefaction strength of decomposed granite soil inferred from array records,

Proc. of the 12th Engineering Mechanics Conf., ASCE, pp.478-481, 1998.

Yamazaki, F., Towhata, I. and Ishihara, K.: Numerical model for liquefaction problem under multi-directional shearing on horizontal plane, *5th Int. Conf. on Numerical Methods in Geomechanics*, Vol.1, pp.339-406, 1985.

Iai,S., Matsunaga, Y. and Kameoka, T. : Strain space plasticity model for cyclic mobility, *Soils and Foundations*, Vol.32, No.2, pp.1-15, 1992.

Yegian, M.K. and Whitman R.V.: Risk analysis for ground failure by liquefaction, *J. of Geotechnical Engineering*, ASCE, Vol.104, pp.921-938, 1978.

Davis, R.O. and Berrill, J.B.: Energy dissipation and seismic liquefaction in sands, *Earthquake Engineering and Structural Dynamics*, Vol.10, pp.59-68, 1982.

Law, K.T. and Cao, Y.L.: An energy approach for assessing seismic liquefaction potential, *Can.*

Geotech. J., Vol.27, pp.320-329, 1990.

Iai, S. *et al.* : Response of a dense sand deposit during the 1993 Kushiro-oki Earthquake, *Soils and Foundations*, Vol.35, No.1, pp.115-131, Mar. 1995.

Schnabel, P.B., Seed, H.B. and Lysmer, J. : SHAKE, A computer program for earthquake response analysis of horizontally layered sites, *Report No. EERC72-12*, Univ. of california, Berkeley, 1972.

Sato,K. *et al.* : Nonlinear seismic response and soil property during strong motion, *Special Issue of Soils and Foundations*, pp.41-52, 1996.